10 Vacuum devices

10.1 INTRODUCTION

In this chapter we consider the interactions which occur between electromagnetic waves and electrons moving in a vacuum. These phenomena have important applications in the generation of high-power radiation at microwave frequencies and above. There is not enough space in this book to discuss the technical details of these devices. The emphasis is on the fundamental processes involved. For greater detail reference should be made to the books and papers listed in the bibliography.

10.2 SPACE-CHARGE WAVES

Many high-power microwave amplifiers depend for their operation upon linear electron beams which are constrained to pass along their axes as shown in Fig. 10.1. The amplification of the devices depends upon the exchange of energy between the electron beam and the electric fields of microwave circuits surrounding it. The equations which govern the motion of the electrons are, first, the continuity equation (1.15)

$$\nabla \cdot \boldsymbol{J} = -\frac{\partial \varrho}{\partial t}, \tag{10.1}$$

where $\boldsymbol{J}$ is the current density and ϱ the charge density; and second, Newton's second law of motion

$$\frac{\mathrm{d}v}{\mathrm{d}t} = \eta(\boldsymbol{E}_\mathrm{c} + \boldsymbol{E}_\mathrm{sc}), \tag{10.2}$$

where η is the charge-to-mass ratio of the electron and $\boldsymbol{E}_\mathrm{c}$ and $\boldsymbol{E}_\mathrm{sc}$ are the electric field applied to the beam and the field arising from the space charge of the electrons. Next we note that the current is related to the charge density and the velocity by

$$\boldsymbol{J} = \varrho v \tag{10.3}$$

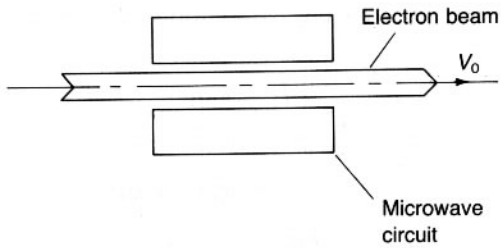

Fig. 10.1 General arrangement of a microwave linear beam tube.

and, finally, the relationship between the charge density and the space-charge field are given by Poisson's equation

$$\nabla \cdot \boldsymbol{E}_\mathrm{sc} = \varrho/\varepsilon_0. \tag{10.4}$$

Note that these four equations involve four dependent variables so, in principle, they can be solved. As a first stage of simplification let us assume that the electrons are moving parallel to the z axis and that the beam extends to infinity in the transverse direction. We will also assume that all quantities vary only with z and with time. The four equations then become

Continuity
$$\frac{\partial J}{\partial z} = -\frac{\partial \varrho}{\partial t}, \tag{10.5}$$

Motion
$$\frac{\mathrm{d}v}{\mathrm{d}t} = \frac{\partial v}{\partial t} + v\frac{\partial v}{\partial z} = \eta(E_\mathrm{c} + E_\mathrm{sc}), \tag{10.6}$$

where the expansion of the left-hand side recognizes that the rate of change of the velocity of the electrons can be expressed as the sum of the rate of change with time at constant position and the rate of change with position as the motion of the electron is followed. The current equation becomes

$$J = \varrho v, \tag{10.7}$$

and Poisson's equation is

$$\frac{\partial E_\mathrm{sc}}{\partial z} = \varrho/\varepsilon_0. \tag{10.8}$$

In these equations the vector quantities $\boldsymbol{J}$, $\boldsymbol{v}$ and $\boldsymbol{E}$ are all assumed to possess only z components. The set of equations is non-linear because (10.7) contains a term which is the product of two variables.

The next stage is to linearize the equations by assuming that all the dependent variables can be written in the form

$$a = a_0 + a_1 \exp \mathrm{j}(\omega t - kz), \tag{10.9}$$

where $a_1 \ll a_0$ and ω and k are the same for all variables. The second term

assumes that the equations have wave solutions. The small-signal equations are then

$$kJ_1 = \omega\varrho_1 \tag{10.10}$$

$$j(\omega - kv_0)v_1 = \eta(E_c + E_{sc}) \tag{10.11}$$

$$J_1 = \varrho_0 v_1 + \varrho_1 v_0 \tag{10.12}$$

and

$$-\mathrm{j}kE_{sc} = \varrho_1/\varepsilon_0. \tag{10.13}$$

For the moment we will assume that the field of the external circuit is zero so that E_{sc} can be eliminated between (10.11) and (10.13) to give

$$(\omega - kv_0)v_1 = \frac{\eta\varrho_1}{k\varepsilon_0}. \tag{10.14}$$

Similarly J_1 can be eliminated between (10.10) and (10.12) to give

$$(\omega - kv_0)\varrho_1 = k\varrho_0 v_1. \tag{10.15}$$

These two equations can be satisfied simultaneously only if

$$(\omega - kv_0)^2 = \eta\varrho_0/\varepsilon_0. \tag{10.16}$$

The terms of this equation have the dimensions of angular frequency squared so we will set

$$\omega_p^2 = \eta\varrho_0/\varepsilon_0. \tag{10.17}$$

The physical significance of this frequency can be understood by considering the case when the electrons have no d.c. component of velocity so that

$$\omega = \omega_p. \tag{10.18}$$

If a stationary cloud of electrons which is in equilibrium is disturbed then it will oscillate with the frequency given by (10.18). Such a cloud of electrons is known as an electron plasma and ω_p is known as the plasma frequency. The possible solutions to (10.16) can therefore be written

$$k_\pm = \frac{\omega \mp \omega_p}{v_0} = k_e \mp k_p. \tag{10.19}$$

It is convenient to display these solutions in the form of a dispersion diagram (see p. 38) as shown in Fig. 10.2. The slope of each line is equal to the d.c. beam velocity v_0. These lines represent two possible wave solutions whose phase velocities are one greater than and the other less than v_0. The waves are compressional charge density waves and are therefore known as fast and slow space-charge waves.

It is often useful to represent these waves by equivalent transmission-line modes. To do this we define an a.c. voltage known as the beam kinetic voltage V_1 by invoking the principle of conservation of energy

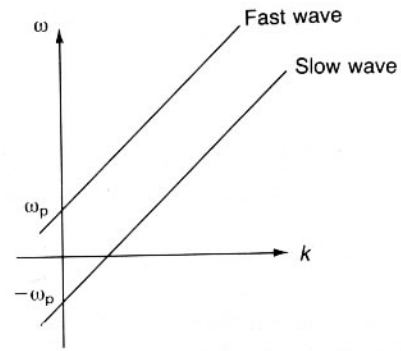

Fig. 10.2 Dispersion diagram of space-charge waves on an electron beam.

$$\tfrac{1}{2}m(v_0 + v_1)^2 = q(V_0 + V_1). \tag{10.20}$$

For small signals the left-hand side can be expanded to give

$$v_0^2 + 2v_0v_1 = 2\eta(V_0 + V_1), \tag{10.21}$$

where the second-order term v_1^2 has been neglected. This equation is true at all times and so the a.c. and d.c. terms must balance separately to give

$$V_1 = v_0v_1/\eta \tag{10.22}$$

and

$$V_0 = v_0^2/2\eta. \tag{10.23}$$

Dividing (10.22) by (10.23) yields

$$\frac{V_1}{V_0} = \frac{v_1}{2v_0}. \tag{10.24}$$

The power density in the waves can then be calculated using the familiar transmission line equation

$$P = \tfrac{1}{2}V_1I_1^*. \tag{10.25}$$

From (10.10) and (10.12) the a.c. current is

$$I_1 = \frac{\omega\varrho_0 A}{(\omega - kv_0)}v_1, \tag{10.26}$$

where A is the cross-sectional area of the beam and, making use of (10.16) and (10.24),

$$I_1 = \frac{2\omega\varrho_0 v_0 A}{\pm\omega_p}\left(\frac{v_1}{2v_0}\right) \qquad \pm\frac{1}{2}\frac{\omega\varrho_0 v_0 A}{\omega_p}\left(\frac{2v_1}{v_0}\right)$$

$$= \pm\frac{2\omega I_0}{\omega_p V_0}\left(\frac{V_1}{V_0}\right) \qquad \pm\frac{1}{2}\frac{\omega}{\omega_p}\frac{I_0}{V_0}V_1 \tag{10.27}$$

so that the power flow in the two waves is

$$P_{\pm} = \frac{1}{2}\frac{|V_1|^2}{Z_{\pm}}, \tag{10.28}$$

where the plus and minus signs refer to the fast and slow space-charge waves, respectively. Their characteristic impedances are given by

$$Z_{\pm} = \pm Z_e = \pm 2\frac{\omega_p}{\omega}\frac{V_0}{I_0}. \tag{10.29}$$

Equation (10.28) reveals the surprising fact that the slow space-charge wave carries negative power. The direction of the power flow is certainly positive because, as Fig. 10.2 shows, the slow wave has a positive group velocity. The explanation of this paradox is to be found in equation (10.27) which shows that in the slow wave the a.c. current and velocity are in antiphase. Thus when $v > v_0$, $J < J_0$, and when $v < v_0$, $J > J_0$. It follows that the average kinetic energy of a beam carrying a slow wave is less than the kinetic energy of an unmodulated beam. In order to set up a slow wave it is necessary to remove power from the beam. This unexpected feature of the slow space-charge wave provides the key to understanding all kinds of microwave linear-beam tubes.

An analysis of the propagation of waves along an electron beam confined by an axial magnetic field shows that there are two other modes which can propagate whose propagation constants are given by

$$k_{\pm} = \frac{\omega \mp \omega_c}{v_0}, \tag{10.30}$$

where $\omega_c = \eta B$ is known as the electron cyclotron frequency. These waves are known as the fast and slow cyclotron waves. They are associated with motion of the electrons in circular orbits around the direction of the axial magnetic field. A fuller discussion of cyclotron modes is given by Louisell (1960).

10.3 KLYSTRON AMPLIFIERS

The arrangement of a simple klystron amplifier is shown schematically in Fig. 10.3. The electron beam passes along the axes of two re-entrant cylindrical resonant cavities. At the centre of each cavity it crosses a gap where it interacts with the alternating electric field of the cavity. Radio-frequency power is fed into the first cavity setting up fields which modulate the velocities of the electrons. To simplify matters we will assume that the length of the gap is short and that at each end the electron beam passes through a grid of fine wires. These grids have the effect of confining all the gap field to the space between them. In practical klystrons grids cannot be

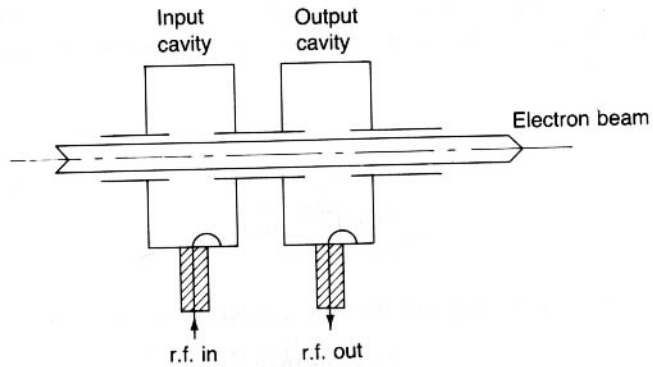

Fig. 10.3 Two-cavity klystron amplifier.

used because they would not be able to withstand the power dissipated in them by the electron beam. It can be shown, however, that gridless gaps can be represented by equivalent gridded gaps for the purposes of analysis.

Figure 10.4 shows a pair of grids d apart with a voltage $V_g\,e^{j\omega t}$ applied across them. To calculate the amplitude of the modulation of the electron velocity we consider an electron which crosses the centre of the gap at the instant when the field is a maximum. Between the grids the electric field is uniform and equal to V_g/d. The equation of motion is then

$$\frac{dv}{dt} = \eta\frac{V_g}{d}e^{j\omega t} \tag{10.31}$$

so that the amplitude of the velocity modulation produced by the gap is

$$v_1 = \frac{\eta V_g}{d}\int_{t_1}^{t_2} e^{j\omega t}\,dt, \tag{10.32}$$

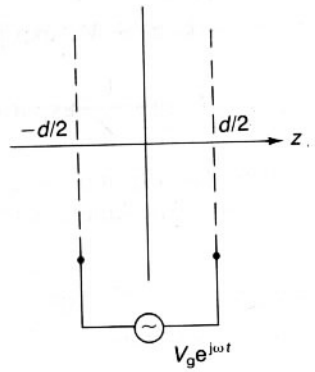

Fig. 10.4 Gridded gap for velocity modulating an electron beam.

where t_1 is the time at which the electron enters the gap and t_2 is the time at which it leaves. If the change in velocity is small compared with the drift velocity v_0 then

$$z = v_0 t \tag{10.33}$$

so that

$$v_1 = \frac{\eta V_g}{v_0 d} \int_{-d/2}^{d/2} e^{jk_e z}\, dz, \tag{10.34}$$

where $k_e = \omega/v_0$. Carrying out the integration we obtain

$$v_1 = \frac{\eta V_g}{v_0} \frac{\sin(k_e d/2)}{k_e d/2}. \tag{10.35}$$

This can be expressed in terms of the beam kinetic voltage by using (10.22) to give

$$V_1 = MV_g, \tag{10.36}$$

where

$$M = \frac{\sin(k_e d/2)}{k_e d/2} \tag{10.37}$$

is known as the gap coupling factor. For an ideal narrow gap $d \to 0$ and $M \to 1$. Physically the coupling factor takes account of the change of the strength of the electric field during the time it takes for an electron to cross the gap. The current is continuous so

$$I_1 = 0. \tag{10.38}$$

Equations (10.36) and (10.38) are the boundary conditions governing the launching of space-charge waves by the gap. Now the general solutions for wave propagation of the beam are

$$V_1 = V_+ \exp j(\omega t - k_+ z) + V_- \exp j(\omega t - k_- z) \tag{10.39}$$

and

$$I_1 = \frac{V_+}{Z_e} \exp j(\omega t - k_+ z) - \frac{V_-}{Z_e} \exp j(\omega t - k_- z), \tag{10.40}$$

where $k_\pm$ and Z_e are given by (10.19) and (10.29). Using the boundary conditions we see that $V_\pm = \frac{1}{2}V_g$. The kinetic voltage and current on the beam are therefore

$$\begin{aligned} V_1 &= \tfrac{1}{2}MV_g(e^{jk_p z} + e^{-jk_p z}) \exp j(\omega t - k_e z) \\ &= MV_g \cos k_p z \exp j(\omega t - k_e z), \end{aligned} \tag{10.41}$$

where $k_e = \omega/v_0$, $k_p = \omega_p/v_0$, and

$$\begin{aligned} I_1 &= -\frac{1}{2}\frac{MV_g}{Z_e}(e^{jk_p z} - e^{-jk_p z}) \exp j(\omega t - k_e z) \\ &= -j\frac{MV_g}{Z_e} \sin k_p z \exp j(\omega t - k_e z). \end{aligned} \tag{10.42}$$

From these two equations it can be seen that as the waves propagate down the beam the amplitudes of the voltage and current modulations change sinusoidally. The wavelength of these standing waves is the plasma wavelength given by

$$\lambda_p = \frac{2\pi}{k_p}. \tag{10.43}$$

Thus, at a distance $\frac{1}{4}\lambda_p$ from the input gap the voltage (i.e. velocity) modulation is zero and the current modulation is a maximum. At this plane the charge density in the beam varies sinusoidally with time and the beam is said to be bunched.

When a bunched beam crosses an interaction gap it induces a current in the gap. The way in which this happens can be understood by considering Fig. 10.5. A bunch of electrons induces positive charges on the grids bounding the gap. As the bunch moves across the gap the induced charges redistribute themselves flowing from one grid to the other through the external load R. The charges shown in the diagram should be regarded as a.c. charges, that is they are charges relative to the d.c. level. Half a cycle later than the situation shown in the diagram the charge in the gap will be less than the d.c. level so it can be thought of as a positive a.c. charge. The induced charges will then be negative and the induced current will flow in the opposite direction.

The flow of induced current through the external load resistor produces a potential difference across the gap and an electric field in the direction shown. This field acts to slow down the electrons in the bunch. The energy removed from the beam is dissipated in the load resistance. This fact enables us to calculate the relationship between the induced current and the

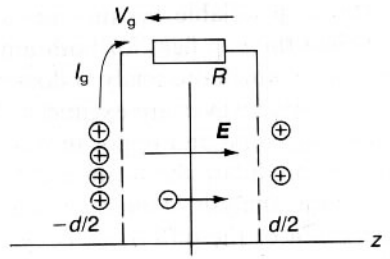

Fig. 10.5 Induction of current by the motion of a bunch of electrons across a gridded gap.

a.c. component of the beam current. At the moment when the centre of the bunch is at the centre of the gap the charge distribution in the gap is given by

$$\varrho(z) = I_1(z)/v_0 \tag{10.44}$$

since the a.c. component of velocity is zero when $\sin k_p z = 1$. From (10.44) we can write

$$\varrho(z) \simeq \frac{|I_1|}{v_0} e^{-jk_e z} \tag{10.45}$$

since $k_p \ll k_e$ so that the sine term in (10.42) is very close to unity. The force on an element of charge within the gap is then

$$F = \int_{-d/2}^{d/2} E_\varrho(z) dz \tag{10.46}$$

so that the rate at which energy is being extracted from the bunch is

$$Fv_0 = \int_{-d/2}^{d/2} E|I_1| e^{-jk_e z}\, dz. \tag{10.47}$$

But this must exactly balance the rate of dissipation of energy in the load given by $I_g V_g$. Thus

$$I_g V_g = \frac{V_g}{d} |I_1| \int_{-d/2}^{d/2} e^{-jk_e z}\, dz \tag{10.48}$$

so that

$$I_g = |I_1| \frac{\sin k_e d/2}{k_e d/2}$$

$$I_g = M|I_1|. \tag{10.49}$$

Thus the gap coupling factor also controls the effectiveness with which the beam drives the gap. It should be noted that the modulated beam behaves as a near-ideal current source.

In the derivation of equations (10.36) and (10.49) we have neglected the space-charge forces. This is justifiable because the space-charge field is normally much smaller than the gap field for both input and output gaps. There is, however, one factor which this analysis does not reveal because it supposes that both space-charge waves are excited with equal amplitudes. Since in that case they carry equal and opposite powers it would appear that no power is needed to modulate the beam and the power gain of the device must be infinite. If the analysis of energy extraction from the beam were repeated taking account of the difference between the space charge waves the result would be

$$I_g = M_+|I_+| + M_-|I_-| \tag{10.50}$$

where

$$M_\pm = \frac{\sin k_\pm d/2}{k_\pm d/2}. \tag{10.51}$$

It can be shown that these coupling factors are also valid for the input gap. The power required to modulated the beam is therefore the difference between the power carried by the two space-charge waves

$$P_{in} = \frac{1}{2Z_c}\left[\left(\frac{M_+ V_g}{2}\right)^2 - \left(\frac{M_- V_g}{2}\right)^2\right]$$

$$= \frac{1}{8}\frac{V_g^2}{Z_c}(M_+^2 - M_-^2). \tag{10.52}$$

Thus the beam appears to the input gap as an impedance

$$R_b = \frac{4Z_c}{M_+^2 - M_-^2}. \tag{10.53}$$

The beam loading of the gaps also has a reactive component which only serves to tune the resonances of the cavities slightly.

The complete two-cavity klystron can be modelled by the equivalent circuit shown in Fig. 10.6. The various resistive components are represented by their conductances ($G = 1/R$). Thus G_s is the source conductance, G_L the load conductance and G_b the beam-loading conductance. The conductance G_c represents the impedance of the cavity resonators. If these are assumed to be tuned to the signal frequency then G_c represents the cavity losses. The magnitudes of the conductances are chosen to give the cavity Q factors appropriate to the bandwidth required. The loaded Q of klystron cavities is typically around 100. The input and output cavities are matched to the source and load when

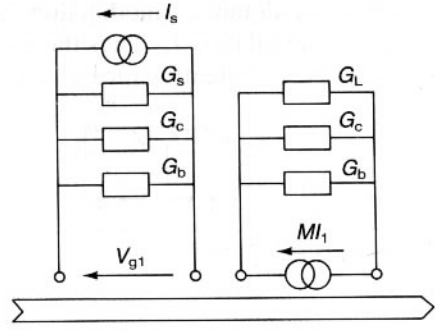

Fig. 10.6 Equivalent circuit of a two-cavity klystron amplifier.

$$G_s = G_c + G_b = G_L. \tag{10.54}$$

The input gap voltage is then

$$V_g = \tfrac{1}{2}I_s/G_s \tag{10.55}$$

and the input power is

$$P_{in} = \tfrac{1}{8}I_s^2/G_s. \tag{10.56}$$

From (10.42) the amplitude of the a.c. beam current at the output gap is

$$|I_1| = MV_g/Z_e \tag{10.57}$$

so that the output power is

$$P_{out} = \tfrac{1}{8}|MI_1|^2/G_s \tag{10.58}$$

whence the power gain is

$$\frac{P_{out}}{P_{in}} = \frac{M^4}{4G_s^2Z_e^2}. \tag{10.59}$$

For typical values of the parameters the gain would be in the region of 15 to 20 dB.

The gain of a klystron can be increased by adding more cavities at intervals of $\lambda_p/4$ as shown in Fig. 10.7. The loads of the second and third cavities do not dissipate much power. Their function is to adjust the Q of the cavities to give the desired bandwidth. The velocity modulation at the input gap produces current modulation I at the second cavity. The induced current in that cavity produces a gap voltage which, in turn, produces a velocity modulation V. Because the electron beam is a linear system at small signal levels this modulation is added to that already on the beam. The gain between the first and second cavities ensures that this modulation is stronger than the initial modulation. At the third cavity the modulation produced by the first cavity appears as pure velocity modulation whilst that from the second cavity produces current modulation I_3. The process here is exactly like that at the second cavity so that a velocity modulation V_3 is added to the beam. This is the dominant modulation at the output cavity where it produces a current modulation I_4. Thus the gain of a multi-cavity klystron can be computed by a straightforward extension of the method

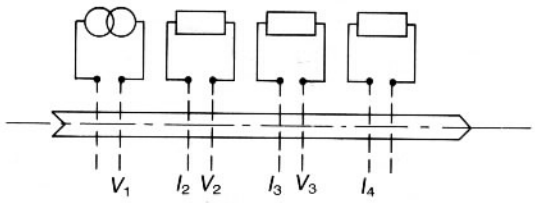

Fig. 10.7 Schematic diagram of a four-cavity klystron amplifier.

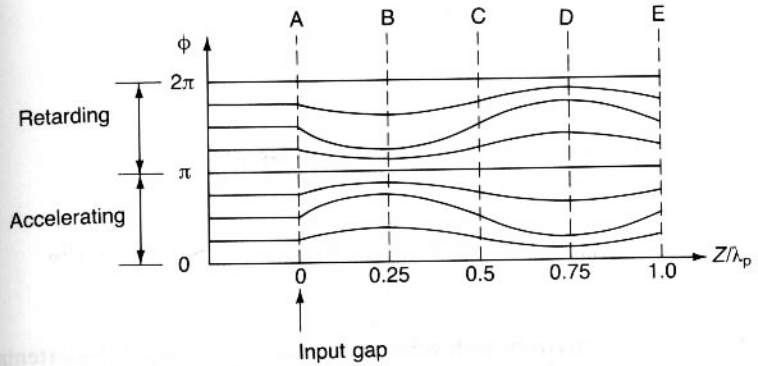

Fig. 10.8 Motion of electrons with velocity modulation relative to the average electron velocity.

described above. The gain at frequencies other than the centre frequency, or when the cavities are not all tuned to the same frequency, can be computed by using matrix algebra to represent the cavities and the drift regions.

The interchange between velocity and current modulation can be represented graphically as shown in Fig. 10.8. This figure shows the phases at which a number of sample electrons cross planes along the length of the beam. The phase is referred to the phase of an electron travelling with the d.c. beam velocity. The slopes of the trajectories show the velocities of the electrons relative to v_0.

At the input gap (A) the trajectories are equally spaced showing no current modulation but their slopes differ because of the velocity modulation produced by the gap field. As the electrons move towards B their trajectories converge. This process is resisted by the repulsive space-charge forces so that at B the trajectories are parallel to the axis. At this plane there is therefore no velocity modulation but a maximum of current modulation. Following the motion forward we see that the space-charge forces cause the trajectories to diverge giving velocity modulation without current modulation at C and so on. From the point of view of an observer travelling with the d.c. beam velocity the electrons are executing oscillations at the plasma frequency about their mean positions. The separation of the planes at which the velocity and current modulations are maximum is therefore equal to $\lambda_p/4$ and is independent of the strength of the modulation.

Clearly it is not possible for this situation to continue at ever higher signal levels. Eventually the process becomes non-linear and the simple theory given above breaks down. This is illustrated by Fig. 10.9. As the signal level increases the plane at which the current modulation is a maximum moves back towards the input gap so the optimum drift length is less than $\lambda_p/4$ (Fig. 10.9(a)). When the signal level is increased still further some of the electron trajectories cross over each other (Fig. 10.9(b)). Once crossing

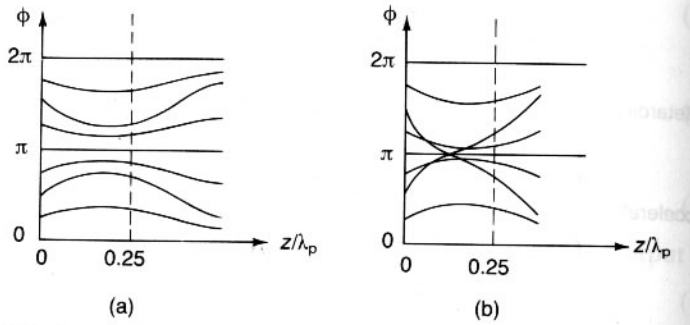

Fig. 10.9 Motion of electrons with velocity modulation showing: (a) shortening of the bunching length, and (b) electron crossovers at high modulation levels.

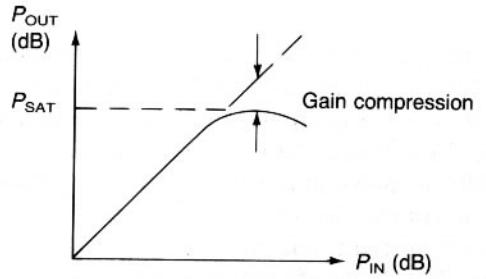

Fig. 10.10 Transfer characteristic of a klystron showing saturation at high drive levels.

over has occurred the effect of the space-charge field is to force the electron still further away from the bunch. This process sets a limit to the maximum bunching which can be achieved and thus to the maximum output power and efficiency of the device. Figure 10.10 shows the typical form of the transfer characteristic of a klystron. At low signal levels the device is a true linear amplifier over a wide dynamic range.

At high signal levels the output saturates as shown. The gain compression at saturation is about 5 dB. For maximum efficiency a klystron must be operated at saturation and this is normal for tubes used for radar transmitters which use an unmodulated carrier. For communications systems such as television transmitters the tube must be operated below saturation in order to avoid non-linear effects.

10.4 SLOW-WAVE STRUCTURES

A klystron works through the interaction between an electron beam and resonant, standing, electromagnetic waves. Travelling-wave tubes (TWTs), on the other hand, employ travelling waves as their name suggests. Because

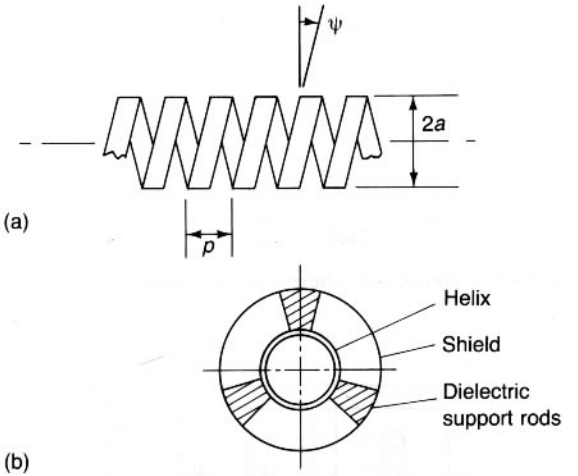

Fig. 10.11 Helix slow-wave structure: (a) elevation and, (b) end elevation.

these waves are non-resonant the interaction can take place over a much wider band of frequencies than in a klystron. In order for an electron beam to interact with a travelling wave it is necessary that the phase velocity of the wave should be approximately the same as the velocity of the electrons.

Waves propagating in a hollow waveguide have phase velocities greater than the velocity of light. They are therefore unsuitable for travelling-wave interactions. To produce a suitable wave we must use a slow-wave structure of which there are two main types.

The first is the helix shown in Fig. 10.11. Modern TWTs generally use a tape helix as shown in Fig. 10.11(a). This helix is mounted within a concentric conducting shield by means of dielectric support rods as shown in Fig. 10.11(b). The result is a rather special kind of coaxial transmission line. At high frequencies the signal follows the turns of the helix travelling at about the velocity of light. The velocity of the wave along the axis is then

$$v_p = c \sin \psi. \tag{10.60}$$

At low frequencies the wave tends to skip from turn to turn of the helix and the phase velocity tends to the velocity of light. Figure 10.12 shows the dispersion diagram for a helical slow-wave structure. The useful bandwidth of such a slow-wave structure is limited by its dispersion at low frequencies and by possible interaction with other modes of the helix for phase shifts greater than about 180° per turn. A bandwidth of an octave is readily attainable. By using dispersion shaping techniques (Webb, 1985) it is possible to make tubes which give useful gain over bandwidths greater than three octaves.

The second main class of slow-wave structure can be thought of as a

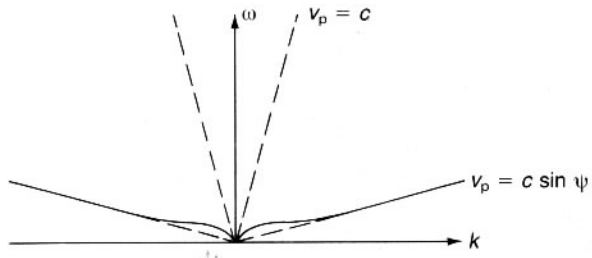

Fig. 10.12 Dispersion diagram of a helix slow-wave structure.

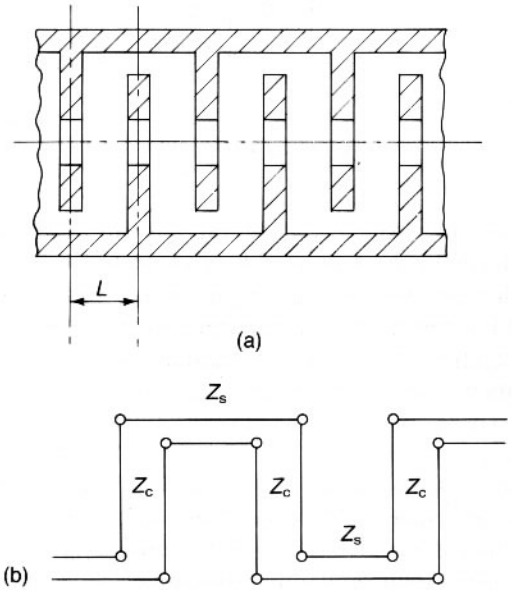

Fig. 10.13 Folded waveguide slow-wave structure: (a) cross-sectional view, and (b) transmission-line equivalent circuit.

folded waveguide as shown in Fig. 10.13(a). The wave travels along the folded guide with a phase velocity greater than the speed of light but its phase velocity in the axial direction is much smaller. This structure can be modelled as a transmission line with alternate sections having different impedances as shown in Fig. 10.13(b). The discontinuities at the junctions between the sections of line produce coupling between the forward and backward waves with stop bands wherever the structure period is an integral number of half wavelengths. The dispersion diagram for a coupled-cavity slow-wave structure of this kind is shown in Fig. 10.14. In this diagram ϕ is the phase shift per section along the folded waveguide. The dispersion

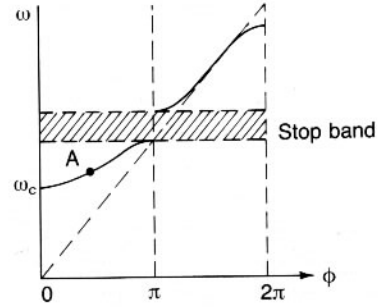

Fig. 10.14 Dispersion diagram of a coupled-cavity slow-wave structure in terms of phase shift along the folded waveguide.

curve is basically the same as that for a hollow waveguide (Fig. 2.16) with propagation at frequencies above the cut-off frequency ω_c. At the edges of the stop band the group velocity is zero. This corresponds to a situation where the effect of reflections at the discontinuities is to produce forward and backward waves of equal amplitude, that is, standing waves. There are two possible standing waves: one with the maximum electric field across the centres of the cavities and the other with the maximum across the centres of the coupling slots as shown in Fig. 10.15. Any general wave can be thought of as a combination of these two normal modes. The two modes have the same wavelength as each other but different frequencies. The relative frequencies depend upon the relative magnitudes of the impedances of the sections of line.

For practical purposes it is the phase shift per cavity along the axis of the

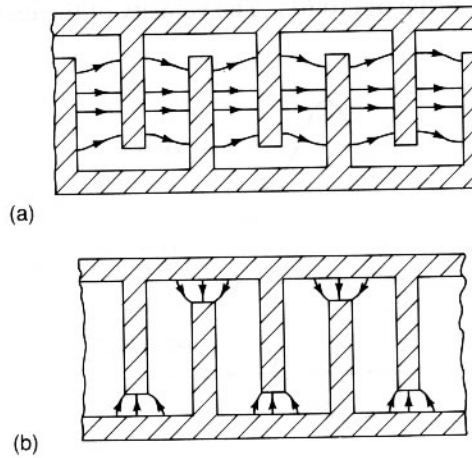

Fig. 10.15 Field patterns at the edges of the stop band in a coupled-cavity slow-wave structure.

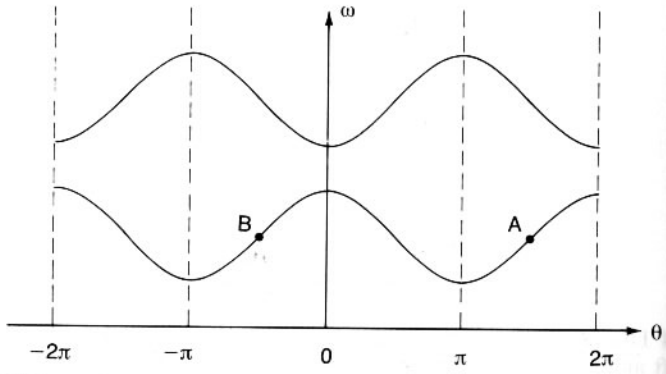

Fig. 10.16 Dispersion diagram of a coupled-cavity slow-wave structure in terms of phase shift per cavity.

slow-wave structure which matters rather than the phase shift along the folded waveguide. A little thought shows that the folding of the waveguide introduces an additional phase shift of 180° per section. Electrons travelling along the axis of the structure experience the interaction field only when they are crossing a cavity. The phase shift perceived by the electrons may therefore be written

$$\theta = \theta_0 + 2n\pi, \tag{10.61}$$

where $n = 0, \pm1, \pm2, \pm3$, etc. and θ_0 is the phase difference between the fields at the centres of adjacent cavities. The dispersion diagram of the slow-wave structure can therefore be plotted in the form shown in Fig. 10.16. The different branches of the dispersion curve are repeated periodically in both directions by virtue of (10.61). The velocity of the electrons is chosen

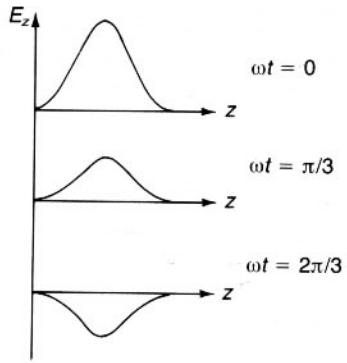

Fig. 10.17 Axial electric field of an interaction gap at different times in the r.f. cycle.

to be synchronous with the circuit wave at the point A where both the group and phase velocities of the circuit wave are positive. The interaction is then similar to that occurring with a helix slow-wave structure.

The significance of the different parts of the curves in Fig. 10.16 becomes clearer if we consider the axial electric field for a particular frequency and phase shift per cavity. Figure 10.17 shows the axial field in one cavity at time intervals corresponding to phase shifts of 60°. If we assume that the phase shift per cavity is also 60° and plot the fields of adjacent cavities the result is a shown in Fig. 10.18. This combination of fields may be expressed as a Fourier series in space and the fundamental component is evidently a wave travelling in the positive z direction as shown by the broken curve in Fig. 10.19(a). At the moment illustrated the magnitude of the field at A is increasing whilst that at B is decreasing both of which are consistent with a fundamental Fourier component travelling to the right.

The next Fourier component is shown in Fig. 10.19(b). From (10.61) this has a phase shift per cavity of −300° ($n = -1$). Consideration of the fields at A and B shows that this wave is travelling in the negative z direction as shown. This is consistent with the negative value of phase shift per cavity computed from (10.61). The wave shown in Fig. 10.19(b) is described as a space-harmonic wave. The complete interaction field can therefore be described in two ways: first as the superposition of a set of standing waves and second as the superposition of a set of travelling space-harmonic waves. For waves propagating in a lossless structure these descriptions are entirely equivalent to each other. In terms of Fig. 10.16 the fundamental waves are in the region $-\pi$ to π whilst the first space-harmonic waves occupy the regions $(-2\pi, -\pi)$ and $(\pi, 2\pi)$. Thus the fundamental forward-wave branch at A in Fig. 10.14 gives rise to a fundamental backward-wave at B in Fig.

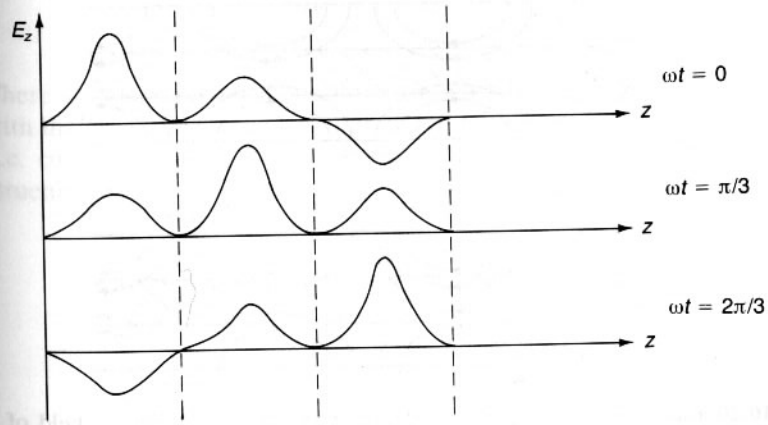

Fig. 10.18 Superposition of the electric fields of adjacent interaction gaps at different times in the r.f. cycle.

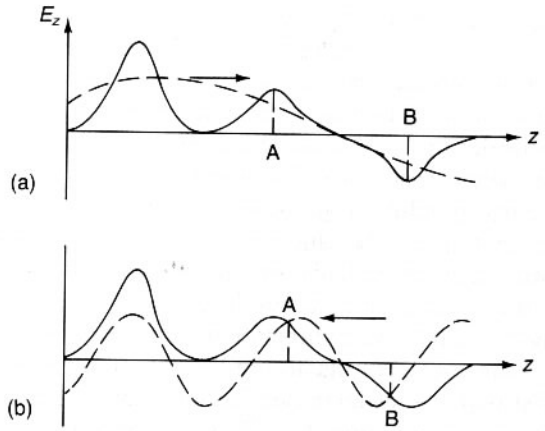

Fig. 10.19 Fourier coefficients of the electric field in a coupled-cavity slow-wave structure: (a) forward-wave fundamental, and (b) backward-wave space harmonic.

10.16 because of the phase reversal introduced by folding the waveguide. The electrons interact with the first forward-wave space-harmonic of that wave at the point A in Fig. 10.16.

10.5 TRAVELLING-WAVE TUBES

Before proceeding to a theoretical analysis of the travelling-wave tube it is useful to obtain a physical understanding of how it works. Figure 10.20(a) shows a uniform stream of electrons which are travelling synchronously

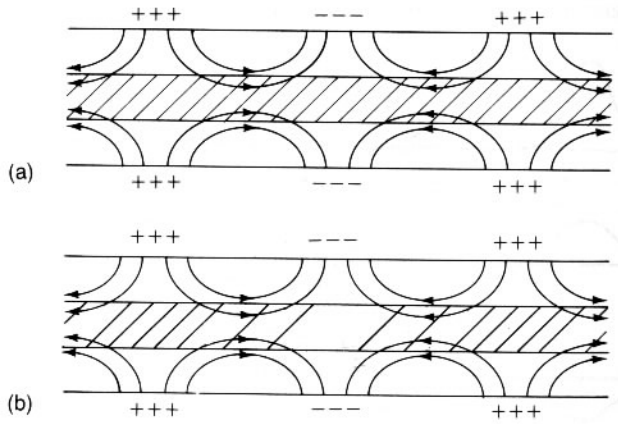

Fig. 10.20 Electron bunching in a travelling wave tube: (a) electric field of the slow-wave structure, and (b) phase relationship between the interaction field and the electron bunches.

with the wave carried by a hypothetical, uniform, slow-wave structure. The electrons are assumed to be constrained by a strong axial magnetic field so that they can only move longitudinally. The fringing field of the slow wave has an axial component of electric field which interacts with the electrons. If the whole system is viewed in a frame of reference which is travelling with the wave then the effect of the interaction is to cause the electrons to become bunched as shown in Fig. 10.20(b). To a stationary observer these current bunches appear as an a.c. current modulation of the electron beam. The electron bunches induce charges on the slow-wave structure which must move along the structure in synchronism with the wave. Moreover, since the bunches are negatively charged, the induced charges have the same polarity as those arising from the original slow wave and add to them to produce growth in the signal level along the length of the tube. The bunching process is limited by the forces of mutual repulsion between the electrons. The principle of conservation of energy requires that the electrons should lose kinetic energy as they transfer power to the wave on the circuit. Eventually this causes the desired synchronous relationship between the electrons and the wave to be lost so that the maximum conversion of energy from d.c. to r.f. is limited.

For the purposes of analysis it is convenient to represent the slow-wave structure by an equivalent transmission line as shown in Fig. 10.21. The inductance and capacitance per unit length of this line can be chosen to make it equivalent to a helix at any given frequency. The propagation of waves on the line coupled to the electron beam are governed by the equations

$$\frac{\partial I}{\partial z} = -C\frac{\partial V}{\partial t} - \frac{\partial i}{\partial z} \tag{10.62}$$

$$\frac{\partial V}{\partial z} = -L\frac{\partial I}{\partial t}. \tag{10.63}$$

There are identical to the usual transmission-line equations (Carter, 1986) with the exception of the last term in (10.62) which reflects the fact that an a.c. current i on the electron beam induces a current on the slow-wave structure and that the total a.c. current on the system must obey Kirchhoff's

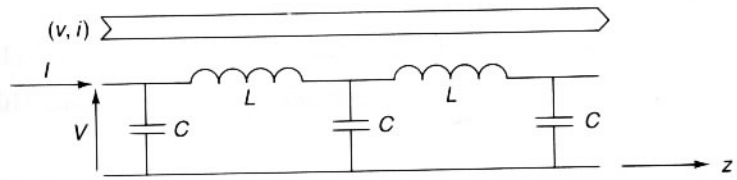

Fig. 10.21 Schematic diagram of a travelling wave tube.

current law. If we assume that waves propagate on the coupled system as $\exp j(\omega t - kz)$ then we obtain

$$jkI = j\omega CV - jki \tag{10.64}$$

$$jkV = j\omega LI \tag{10.65}$$

and, eliminating I, we obtain

$$V = \frac{kk_0Z_0}{k_0^2 - k^2} i, \tag{10.66}$$

where

$$k_0 = \omega\sqrt{(LC)} \tag{10.67}$$

is the natural propagation constant for waves on the line in the absence of the electron beam and

$$Z_0 = \sqrt{(L/C)} \tag{10.68}$$

is the characteristic impedance of the line. Notice that the inductance and capacitance per unit length have been replaced by quantities which have more meaning at microwave frequencies.

The interaction field is related to the voltage on the line by

$$E_c = -\frac{\partial V}{\partial z} = jkV \tag{10.69}$$

so that

$$E_c = j\frac{k^2k_0Z_0}{k_0^2 - k^2} i. \tag{10.70}$$

A second relationship between the a.c. current on the beam and the a.c. circuit voltage can be derived by considering the electron beam dynamics starting from equations (10.10) to (10.13). Eliminating ϱ_1 from (10.10) and (10.12) and from (10.10) and (10.13) yields

$$(\omega - kv_0)J_1 = \omega\varrho_0 v_1 \tag{10.71}$$

and

$$E_{sc} = j\frac{J_1}{\omega\varepsilon_0}. \tag{10.72}$$

We also have

$$j(\omega - kv_0)v_1 = \eta(E_c + E_{sc}). \tag{10.11}$$

Eliminating the space-charge field and the a.c. velocity from (10.11), (10.71) and (10.72) gives

$$J_1 = \frac{j\omega v_0}{\omega_p^2 - (\omega - kv_0)^2}\frac{J_0E_c}{2V_0} \tag{10.73}$$

and integrating across the cross sectional area of the electron beam gives

$$i = \frac{j\omega v_0}{\omega_p^2 - (\omega - kv_0)^2}\frac{I_0E_c}{2V_0} \tag{10.74}$$

in which the d.c. and a.c. currents replace the corresponding current densities.

For self consistency equations (10.66) and (10.74) must be satisfied simultaneously so that the possible values of the propagation constant k are given by

$$[k_0^2 - k^2][k_p^2 - (k_e - k)^2] = -k_ek_0k^2\frac{I_0Z_0}{2V_0}. \tag{10.75}$$

This equation is known as the determinantal equation of the system. If the coupling term on the right-hand side of the equation is set to zero the roots are

$$k = \pm k_0 \tag{10.76}$$

(the forward and backward waves on the transmission line) and

$$k = k_e \pm k_p \tag{10.77}$$

(the fast and slow space-charge waves on the electron beam). These solutions are shown in the dispersion diagram in Fig. 10.22. The interaction which produces gain is that at A between the forward circuit wave and the slow space-charge wave. We have already remarked that the slow space-charge wave is excited by removing energy from the electron beam. It is therefore possible for energy to be transferred from this wave to the wave on the slow-wave structure in such a way that both grow with distance.

The full solution of the coupled equation (10.75) requires the use of a computer but a useful approximation can be derived by assuming that only coupling between the slow space-charge wave and the forward circuit wave

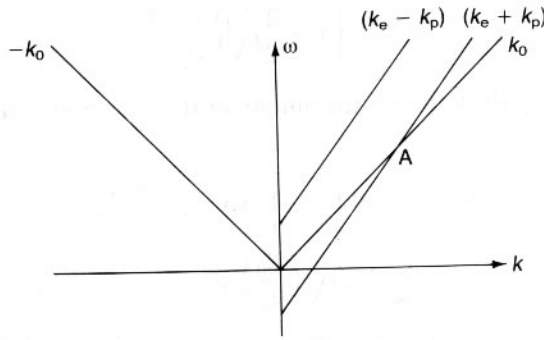

Fig. 10.22 Dispersion diagram of the uncoupled slow-wave structure and electron beam modes in a helix travelling-wave tube.

is important. First (10.75) is rewritten with the left-hand side expressed as a product of four factors and the right-hand side rewritten in terms of the beam characteristic impedance Z_e (10.29) to give

$$(k_0 - k)(k_0 + k)(k_p - k_e + k)(k_p + k_e - k) = -k_e k_0 k k_p \frac{Z_0}{Z_e}. \quad (10.78)$$

This can be rearranged to keep only the two roots in which we are interested on the left-hand side

$$(k - k_0)(k - k_p - k_e) = -\left(\frac{kk_0}{k + k_0}\right)\left(\frac{k_e k_p}{k - k_e + k_p}\right)\frac{Z_0}{Z_e}. \quad (10.79)$$

Now we know that the roots of this equation must lie close to the roots of the left-hand side, namely $k = k_0$ and $k = k_e + k_p$. We therefore approximate the two brackets on the right-hand side of the equation by substituting the two roots into them in the same order. The result is

$$(k - k_0)(k - k_p - k_e) = -\frac{k_0 k_e}{4}\frac{Z_0}{Z_e}. \quad (10.80)$$

This equation can be solved by the usual method to give

$$k = \tfrac{1}{2}(k_0 + k_p + k_e) \pm \tfrac{1}{2}[(k_0 - (k_p + k_e))^2 - k_0 k_e Z_0/Z_c]^{\frac{1}{2}}. \quad (10.81)$$

The solution reveals a number of important things about the travelling wave tube interaction.

If the term under the square root is negative k has a pair of complex conjugate roots. These correspond to a pair of waves one of which grows exponentially with distance whilst the other decays. The real part of both these roots is given by the first term which is just the mean of the two uncoupled roots.

At synchronism $k_0 = k_e + k_p$ and (10.81) becomes

$$k = k_0\left[1 \pm \frac{1}{2}j\sqrt{\left(\frac{Z_0}{Z_e}\right)}\right]. \quad (10.82)$$

The imaginary part is then a maximum so the maximum gain per wavelength is given by

$$\text{Gain} = 20\log_{10}\left[\exp \pi\sqrt{\left(\frac{Z_0}{Z_e}\right)}\right] = 27.3\sqrt{\left(\frac{Z_0}{Z_e}\right)}\,\text{dB}. \quad (10.83)$$

Typically Z_e is 50 to 100 times Z_0 giving a gain of around 3 to 4 dB per wavelength. It is not surprising that high gain is obtained with high values

of Z_0, corresponding to a high interaction field for a given power flow, and low Z_e, corresponding to a high-current electron beam.

The bandwidth of the interaction can be deduced by considering the points at which the imaginary part of (10.80) becomes zero, that is

$$\frac{k_0 - (k_p + k_e)}{\sqrt{(k_0 k_e)}} = \sqrt{\left(\frac{Z_0}{Z_e}\right)}. \quad (10.84)$$

The left-hand side of this expression is the normalized difference between the propagation constants of the uncoupled waves. This increases with the square root of the ratio of the circuit impedance to the beam impedance. Figure 10.22 shows that for a given value of this ratio the bandwidth increases as the angle between the two intersecting lines decreases, that is, as synchronism is maintained over a broader band of frequencies. In practice these requirements tend to conflict as broad-band slow-wave structures have low impedances.

The information deduced in the preceding paragraphs enables us to sketch the form of the dispersion diagram for the coupled system. This takes the form shown in Fig. 10.23 with complex conjugate roots and gain in the frequency range $\omega_1 < \omega < \omega_2$.

The theory of the coupled-cavity travelling-wave tube takes a slightly different form because the interaction between the beam and the wave is lumped rather than continuous. Figure 10.24 shows the coupled-mode diagram for a coupled-cavity TWT. The mid-band gain of such a tube can be estimated fairly accurately from (10.83) if the impedance of the correct space harmonic is substituted for Z_0. The analogy with the continuous interaction breaks down at low values of phase shift per cavity when the excitation of a backward wave becomes important.

Helix TWTs typically have working bandwidths in the range from one to

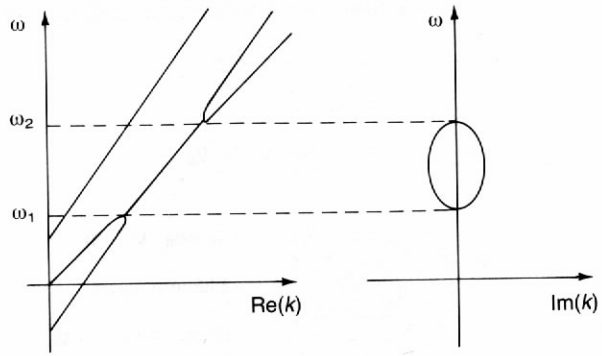

Fig. 10.23 Dispersion diagram of a travelling-wave tube showing the presence of a complex conjugate pair of roots produced by the interaction between the slow space-charge wave and the forward wave on the helix.

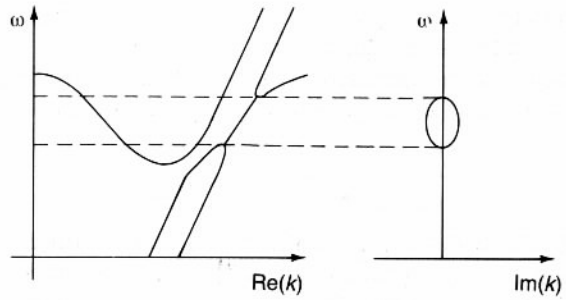

Fig. 10.24 Dispersion diagram for a coupled-cavity travelling-wave tube in which the slow space-charge wave interacts with the first space harmonic of the wave on the slow-wave structure.

three octaves. At 10 GHz mean powers of a few hundred watts and peak, pulsed, powers of a few kilowatts can be obtained. Coupled-cavity TWTs operate over narrower bands (around 15%) because of the greater dispersion of coupled-cavity slow-wave structures. However they have much better heat dissipation capabilities than helices so that a mean power of 10 kW and a peak power of several hundred kilowatts, or more, at 10 GHz are readily achieved. Further information about travelling-wave tubes can be found in Gilmour (1986).

10.6 CROSSED-FIELD TUBES

The linear-beam tubes (klystrons and TWTs) described so far all rely for their operation on a linear electron beam which is confined by some arrangement of axial magnetic field. This is not the only way to get electrons to flow in a smooth controlled manner. A possible alternative is to use crossed electric and magnetic fields as shown in Fig. 10.25(a) with the electric field

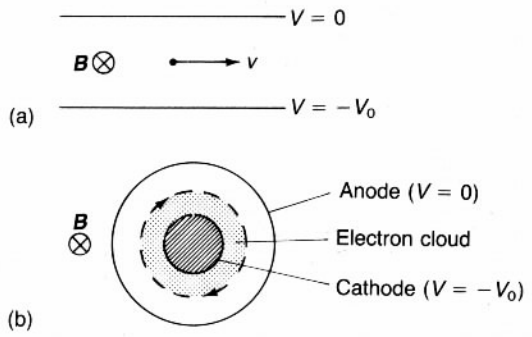

Fig. 10.25 Crossed-field electron flow: (a) linear geometry, and (b) cylindrical geometry.

produced by a pair of plane parallel electrodes. Here the electric and magnetic forces balance and the electron moves in a straight line parallel to the electrodes. In practice it is convenient to make the electrodes concentric cylinders so that the electrons move in regular circular orbits. The addition of space charge does not materially affect the electron flow so it is possible to produce a rotating electron cloud as shown in Fig. 10.25(b). Provided that the magnetic field is strong enough the electrons do not reach the anode and the diode is cut off. The electrons are usually emitted from the whole of the cathode surface through a combination of thermionic and secondary emission.

By arranging that the surface of the anode is a slow-wave structure it is possible to envisage interactions with the electrons analagous to those taking place in a TWT. The mathematical analysis of this kind of device is difficult and they normally operate in the non-linear regime anyway so we will concentrate on the physical principles of operation.

The commonest device of this kind is the magnetron oscillator in which the slow-wave structure is made in the form of a closed circle as shown in Fig. 10.26. The anode and cathode together form a two-conductor transmission line which can propagate TEM waves at the velocity of light and at frequencies down to d.c. The forward and backward waves are coupled by the discontinuities in the structure and are most strongly coupled at a frequency close to that at which the spaces between the vanes are resonant. The result, as in coupled-cavity TWT structures, is to produce a pattern of pass and stop bands as shown in Fig. 10.27. Because the slow-wave structure is closed upon itself the possible frequencies of oscillation are limited to those for which there is a whole number of wavelengths around the perimeter of the device. The possible resonances in the lowest mode are shown in Fig. 10.27 for an eight-vane anode like that in Fig. 10.26. The flat top of the dispersion curve means that most of the resonances are grouped within a very narrow frequency band.

Of all the possible resonances only that for which the phase shift per

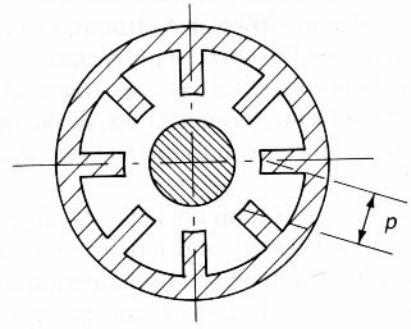

Fig. 10.26 Cross section of a magnetron anode.

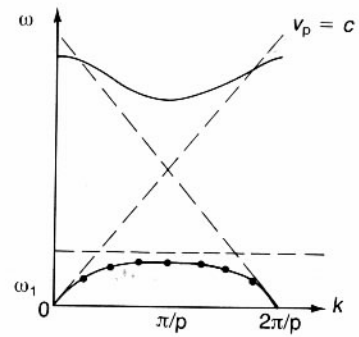

Fig. 10.27 Dispersion diagram of an eight-cavity magnetron anode showing the resonant frequencies.

cavity is 180° has a field pattern which is locked to the orientation of the anode vanes. This 'π mode' is therefore the one chosen for the interaction. When the magnetron is turned on the electrons may interact with other modes besides the π mode particularly the next nearest modes on either side. The interaction starts from the thermal noise in the device and the different modes compete until eventually one becomes dominant. An important part of magnetron design is ensuring that the correct mode is always excited to the exclusion of others. This is achieved by careful design of the anode to get the greatest possible separation between the π mode and the unwanted modes and by tailoring the shape of the voltage pulse applied between cathode and anode to assist anode the growth of the π mode.

In common with other oscillators the magnetron can be locked to a particular phase and frequency by the injection of a signal within the anode resonance Q curve at a level about 10 dB below the output power of the device. A next stage in this train of thought is to make a break in the slow-wave structure, so that it is no longer resonant, and to couple the ends to external waveguides as shown in Fig. 10.28. This device can act as an amplifier employing either a forward-wave or backward-wave interaction depending upon the type of slow-wave structure employed. It does not show the kind of linear, small-signal, amplification found in linear beam tubes and is probably best thought of as a special kind of locked oscillator with a wider range of operating frequencies than the magnetron. The gain is usually only 10 to 20 dB in contrast to the 40 to 60 dB commonly achieved by linear-beam tubes.

Crossed-field devices possess a number of advantages over linear-beam tubes. First, they are much lighter and more compact for a given power output and frequency. Second they can operate at lower impedances (low voltage, high current) and, third, they are intrinsically more efficient converters of d.c. input to r.f. output power. The last property arises because

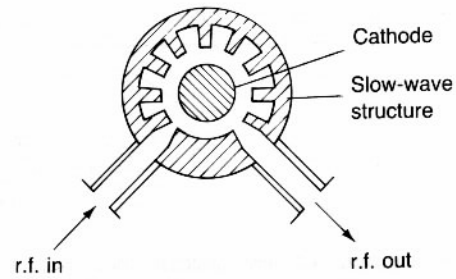

Fig. 10.28 Arrangement of the slow-wave structure of a cross-field amplifier.

the electrons move gradually closer to the anode as they interact with the wave on the structure. Their kinetic energy is thus replenished from the d.c. electric field as fast as it is converted to r.f. power. The electrons therefore remain in synchronism with the wave throughout the interaction. Magnetrons with conversion efficiencies of over 80% have been made for applications such as industrial heating where efficiency is a prime consideration. For further information on crossed-field devices see Gilmour (1986).

10.7 FAST-WAVE DEVICES

All the devices described so far in this chapter depend for their operation upon slow-wave structures or resonant cavities. These features scale linearly with wavelength and become increasingly difficult and expensive to make as the required frequency and power increase. The upper frequency limit for conventional slow-wave devices is around 100 GHz. Alternative approaches which do not require the use of delicate microwave structures have been the subject of much research in recent years because of their potential for generating large amounts of power at sub-millimetre wavelengths.

In a coupled-cavity TWT it is possible to work at beam velocities well below the speed of light by making use of the space harmonics of the wave on the slow-wave structure. This suggests that useful interaction could be obtained by using an electron beam which varies periodically in some fashion so that the interaction is between a fast electromagnetic wave in a waveguide and a space harmonic of the electron beam modes.

Figure 10.29 shows one possible way of achieving this result. A thin high-velocity electron beam confined by an axial magnetic field is directed down the centre of a rectangular waveguide. The beam is deflected alternately to the right and left of the mid-plane by the periodic transverse magnetic field of a 'wiggler'. Each time the direction of transverse motion of an electron is reversed it experiences an acceleration and therefore emits electromagnetic radiation over a broad band of frequencies. If the ends of the waveguide

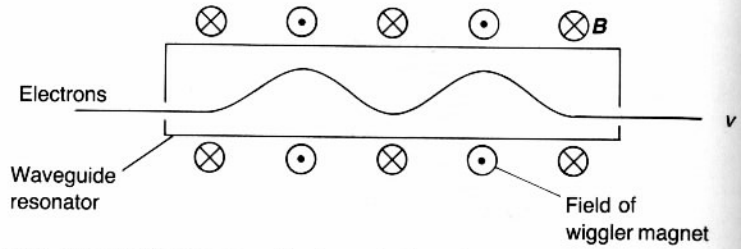

Fig. 10.29 Schematic diagram of a free-electron laser.

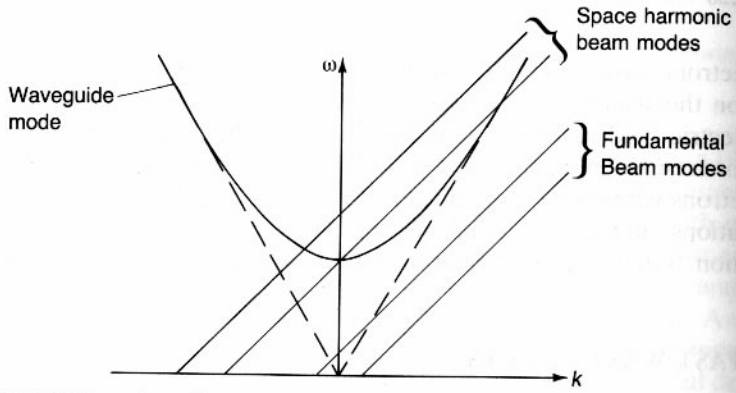

Fig. 10.30 Dispersion diagram showing the interaction between a space-harmonic of the waves on a periodic electron beam and a fast waveguide mode.

are closed so that it becomes resonant then the radiation from the electrons is stimulated by the standing wave in the resonator. The resemblance between this situation and that in a laser has led to the description of this device as a 'free electron laser' (FEL). An alternative view is that the interaction is represented by the dispersion diagram shown in Fig. 10.30 which shows the synchronism between the fast electromagnetic wave in the waveguide and a space harmonic of the slow cyclotron mode on the electron beam. FELs have, so far, only been constructed as experimental devices making use of the intense, high-energy, beams generated by electron accelerators. In one experiment pulsed powers of up to 1 GW were obtained at 35 GHz. In another it has been demonstrated that electromagnetic powers at optical wavelengths can be produced.

An alternative arrangement, shown in Fig. 10.31, has a hollow relativistic electron beam directed along a circular waveguide. The electrons interact with the field of the TE_{01} (circular electric) mode of the waveguide at the cyclotron frequency. They are arranged at the radius where the field strength of that mode is a maximum. Within the beam individual electrons describe orbits as shown in Fig. 10.32. The radius of an orbit is given by

$$r = v_\perp/\omega_c \tag{10.85}$$

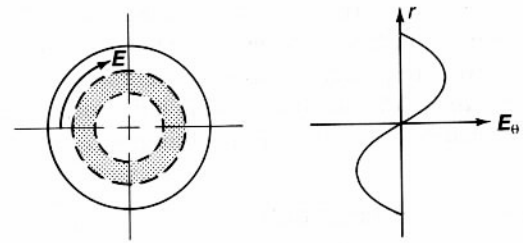

Fig. 10.31 The arrangement of a hollow electron beam in a cylindrical waveguide used in gyrotrons.

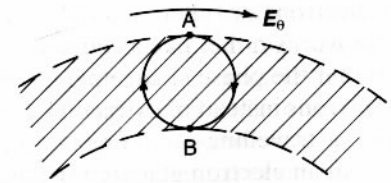

Fig. 10.32 Gyrotron interaction between the tangential component of the r.f. field and an electron moving in a small orbit within the electron beam.

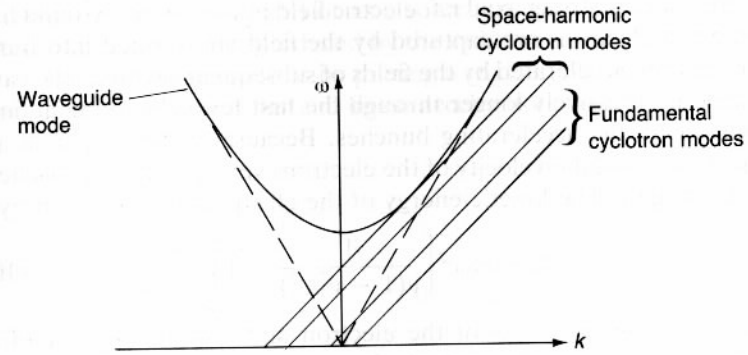

Fig. 10.33 Dispersion diagram of a gyrotron oscillator.

where $v_\perp$ is the tangential velocity of the electron and the relativistic cyclotron frequency is given by

$$\omega_c = \frac{\eta B_0}{\gamma(1 - v^2/c^2)}. \tag{10.86}$$

An electron at the point A is accelerated by the field so its cyclotron frequency increases. Conversely an electron at B is retarded so that its cylotron frequency decreases. The effect of this is that the electrons are bunched by the field and can give up energy to it. This is an interaction between the fast cyclotron mode on the beam and the fast electromagnetic wave in the waveguide as shown in Fig. 10.33. Devices which work on this

principle are known as cyclotron resonance masers (CRMs) or gyrotrons. Gyrotrons have been constructed which provide 100 kW of pulsed power at 200 GHz. At lower frequencies pulsed powers in excess of a megawatt and mean powers of 75 kW has been achieved. Further information on fast-wave devices can be found in Granatstein and Alexeff (1987).

10.8 ELECTRON ACCELERATORS

The devices described in the earlier parts of this chapter are all concerned with the conversion of the energy of moving electrons into radiofrequency power. It is, however, possible to reverse the processes in order to produce beams of high-energy electrons or other charged particles.

The linear accelerator works rather like a coupled-cavity travelling-wave tube. The difference is that the phase change per cavity is chosen to accelerate the bunches of electrons instead of extracting energy from them. The general arrangement of a travelling-wave linear accelerator is shown in Fig. 10.34. Electrons from an electron gun are injected into the first cavity of a chain of coupled cavities. The cavities are generally coupled together by the axial hole through which the electrons pass. Radiofrequency power is fed in to the cavity chain from a high-power source such as a magnetron to provide a very strong axial r.f. electric field in the cavity. Around half of the injected electrons are captured by the field and formed into bunches which are then accelerated by the fields of subsequent cavities. The cavities are made progressively longer through the first few cells to maintain synchronism with the accelerating bunches. Because of the very high accelerating fields used the velocity of the electrons very quickly approaches the velocity of light. The kinetic energy of the electrons is then given by

$$E = m_0c^2\left[\frac{1}{\sqrt{(1 - v^2/c^2)}} - 1\right], \qquad (10.87)$$

where m_0 is the rest mass of the electron and c is the velocity of light (Rosser, 1964). As the electron velocity approaches the velocity of light the

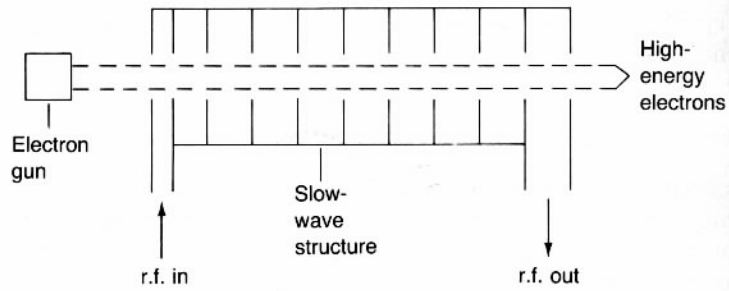

Fig. 10.34 Schematic diagram of a microwave linear accelerator.

kinetic energy becomes very large. Thus, after the first few cells, the effect of the accelerating field is to increase the energy of the electrons without appreciably increasing their velocities. The energies of the electrons are usually expressed in terms of electron volts (the energy gained by an electron in moving through a potential difference of one volt). The electron energies produced by linear accelerators vary from a few MeV for accelerators used for radiotherapy to the 20 GeV of the two-mile accelerator at Stanford in California.

When very high-energy electrons are required from a more compact source a synchrotron may be used. This machine has the general arrangement shown in Fig. 10.35. Electron bunches are formed by a linear accelerator and injected into a beam tube which forms a closed loop. Straight sections of the tube are separated by bending magnets whose strength can be adjusted to keep the bunches moving along the centre of the beam tube as their energy increases. One or more microwave cavities very like those used in klystrons are inserted into the beam tube. The synchrotron is designed in such a way that the bunches experience an accelerating field each time they cross a cavity. Because the electron velocity is very close to the speed of light the time taken for a bunch to go once around the ring is virtually constant. A synchrotron may be used as a source of high-energy electrons (typically a few GeV) or as a source of intense electromagnetic radiation. This radiation is produced by the radial acceleration of the electrons in the bending magnets or by putting a wiggler magnet in one of the straight sections. Synchrotrons and linear accelerators have both been used

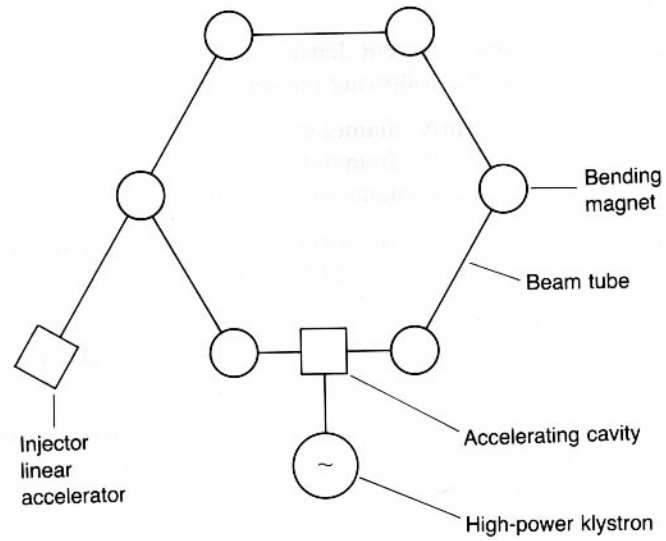

Fig. 10.35 Schematic diagram of a synchrotron storage ring.

to provide the high-energy electrons required for experiments with free-electron lasers.

10.9 CONCLUSION

In this chapter we have considered some of the interactions which take place between free electrons and electromagnetic waves. These interactions are fundamental to the operation of high-power microwave sources and to particle accelerators. Closely related phenomena occur in ionized gasses including the plasmas used in experiments on nuclear fusion.

Streams of electrons carry space-charge and cyclotron waves and these can interact with external r.f. fields to produce amplification. The beating between the fast and slow space-charge waves is used in the klystron. The interaction between the slow space-charge wave and the wave on a slow-wave structure is fundamental to the operation of the travelling-wave tube and the magnetron oscillator.

Newer devices such as the gyratron and the free-electron laser employ interactions between electrons and fast electromagnetic waves in waveguides. These devices hold the promise of generation of very large amounts of power at wavelengths ranging from millimetres down to optical wavelengths.

The interaction between charged particles and radiofrequency electric fields is employed in linear accelerators, synchrotrons and other particle accelerators to produce particle energies ranging from MeV to GeV.

EXERCISES

10.1 Calculate the velocity, current density and plasma frequency for electron beams having the following parameters:

1. $V = 5\,\text{kV}$, $I = 20\,\text{mA}$, diameter $= 1\,\text{mm}$,
2. $V = 10\,\text{kV}$, $I = 0.5\,\text{A}$, diameter $= 5\,\text{mm}$,
3. $V = 60\,\text{kV}$, $I = 12\,\text{A}$, diameter $= 8\,\text{mm}$.

(Note: at high voltages the beam velocity must be calculated using the relativistically correct equation (10.87) in place of (10.23).)

10.2 Calculate the plasma wavelength and the electronic wavelength and characteristic impedance at 3 GHz, 10 GHz and 60 GHz for each of the beams defined in Question 10.1.

10.3 Calculate the d.c. power and the fast- and slow-wave powers at 10 GHz for each of the beams in Question 10.1 if the beam kinetic voltage is 10% of the d.c. voltage in each case.

10.4 Calculate the gain at 10 GHz and the bandwidth of a two-cavity klystron amplifier whose electron beam has the parameters given in Question 10.1 part 1. The cavities have unloaded Q factors of 500 and R/Q of 800 Ω and the gap transit angles ($k_e d$) are $\pi/2$.

10.5 The electron beam defined in Question 10.1 part 1 is used in a helix travelling-wave tube with a centre frequency of 10 GHz. Calculate the pitch angle of the helix and the gain of a section of tube 30 mm long if the interaction impedance of the helix is 500 Ω.